TAT Peptide and Its Conjugates: Proteolytic Stability

Jacob Grunwald,[¶,†] Tomas Rejtar,[‡] Rupa Sawant,[†] Zhouxi Wang,[‡,§] and Vladimir P. Torchilin*[,†]

Department of Pharmaceutical Sciences and Center for Pharmaceutical Biotechnology and Nanomedicine, Barnett Institute and Department of Chemistry and Chemical Biology, Northeastern University, Boston, Massachusetts 02115. Received February 20, 2009; Revised Manuscript Received June 19, 2009

The proteolytic cleavage of TATp, TATp-PEG_{1000}-PE conjugate (TATp-conjugate), and TATp as TATp-conjugate in mixed micelles made of TATp-conjugate and PEG_{5000}-PE (2.5% mol of TATp-conjugate, TATp-Mic) were studied by HPLC with fluorescent detection using fluorenylmethyl chloroformate (FMOC) labeling and by MALDI-TOF MS analysis. The cleavage kinetics were analyzed in human blood plasma and in trypsin-containing phosphate buffered saline (PBS), pH 7.4, to simulate the proteolytic activity of human plasma. The trypsinolysis of free TATp, TATp-conjugate, and TATp-Mic revealed that the main initial fragmentation is an endocleavage at the carboxyl terminus resulting in an Arg-Arg (RR) dimer. The trypsinolysis followed pseudo-first-order kinetics. The cleavage of the free TATp was relatively fast with a half-life of a few minutes ($t_{1/2} \sim 3.5$ min). The TATp-conjugate showed more stability with about a 3-fold increase in half-life ($t_{1/2} \sim 10$ min). TATp in TATp-Mic was highly protected against proteolysis with an over 100-fold increase in half-life ($t_{1/2} \sim 430$ min). The shielding of TATp by PEG moieties in the proposed TATp-Mic is of great importance for its potential use as a cell-penetrating moiety for multifunctional "smart" drug delivery systems with detachable PEG.

INTRODUCTION

Cell-penetrating peptides (CPPs) are molecules commonly of a polycationic nature. They readily cross the hydrophobic cell membrane (*1–5*) and can facilitate intracellular delivery of conjugated macromolecules and nanoparticles. The mechanism of their activity is not yet completely elucidated (*6–11*), although it is assumed that CPPs themselves and CPPs with a small-sized cargo cross the cell membrane via a combination of hydrophobic and electrostatic interactions (*12*), while CPPs with a large-sized cargo enter cells via macropinocytosis with subsequent escape from endosomes (*13*). In the past decade, numerous works have been published on the use of CPPs for successful *in vitro* and *in vivo* intracellular delivery of biologically active macromolecules (*14–16*), enzymes (*3*), antibodies (*15*), DNA (*17–19*), liposomes (*20–22*), and imaging probes (*3, 23–25*). The most intensively studied CPP is the transactivating transcriptional activator peptide (TATp) derived from the protein transduction domain (PTD) of HIV-1 (*1, 2, 26, 27*) extending from residues 47 to 57 (YGRKKRRQRRR). The composition of TATp is unique for its predominant content of the positively charged amino acids arginine and lysine. This distinct composition makes it highly susceptible to proteolysis by tryptic enzymes. As pointed out in a recent review (*6*), TATp has six potential trypsin cleavage sites. Since the cell penetration property relies on the integrity of the highly basic TATp sequence (*6, 7*), it is clear that the potential of TATp or similar peptides as mediators of intracellular delivery of therapeutic molecules and drug delivery systems *in vivo* could be significantly limited by their cleavage with proteolytic enzymes (*28–31*).

Despite the enormous number of publications on the use of TATp as a mediator of intracellular delivery, only a few authors have investigated the *in vivo* instability of TATp (*28*) that results from its proteolytic cleavage (*28, 29*). To obtain stable CPPs, an all D-enantiomer peptide was suggested (*30, 31*); another approach offered to overcome proteolytic degradation (*32, 33*) was the replacement of the amino acids, which are particularly susceptible to degradation, with their stable synthetic mimics.

In the study specifically dedicated to the enzymatic cleavage of TATp (*28*), the investigation of furin cleavage of HIV-1 TATp showed that cleavage takes place at the carboxyl terminus and greatly reduces its transactivation activity. However, no studies have been done to determine the kinetics of the proteolysis of TATp or fragment identification by MS.

Our aim was to study the exact pattern of TATp proteolysis and compare the stability against proteolysis (trypsinolysis) of different forms of TATp: native TATp, TATp conjugated with poly(ethylene glycol)-phosphatidyl ethanolamine block copolymer (TATp-PEG-PE), and TATp as TATp-PEG-PE incorporated into PEG-PE micelles with the PEG block in the PEG-PE longer than the PEG block in TATp-PEG-PE conjugate. The kinetics of the proteolytic cleavage of TATp in these forms were investigated using HPLC with fluorescent labeling and MALDI-TOF-MS.

EXPERIMENTAL SECTION

Chemicals. TATp (11-mer: TyrGlyArgLysLysArgArgGlnArgArgArg; molecular mass 1560 Da) and TAT-cysteine peptide (TATp-Cys 12-mer: CysTyrGlyArgLys-LysArgArgGlnArgArgArg; molecular mass 1663 Da, one reactive thiol group) were synthesized by the Tufts University Core Facility (Boston, MA). 1,2-Dioleoyl-*sn*-glycero-3-phosphoethanolamine (DOPE) and 1,2-dioleoyl-*sn*-glycero-3-phosphoethanolamine-*N*-[methyl(poly(ethylene glycol))-5000] (PEG_{5000}-PE) were purchased from Avanti Polar Lipids Inc. (Alabaster, AL), NHS-PEG_{1000}-maleimide was purchased from Quanta Biodesign (Powell, OH), and

* Corresponding author. Dr. Vladimir P. Torchilin, Department of Pharmaceutical Sciences, Northeastern University, Mugar Building, Room 312, 360 Huntington Avenue, Boston, MA 02115. tel 617-373-3206; fax 617-373-8886, e-mail: v.torchilin@neu.edu.

¶ While on leave from Israel Institute for Biological Research, Ness Ziona, Israel.

† Department of Pharmaceutical Sciences and Center for Pharmaceutical Biotechnology and Nanomedicine.

‡ Barnett Institute.

§ Department of Chemistry and Chemical Biology.

10.1021/bc900081e CCC: $40.75
Published on Web 07/14/2009

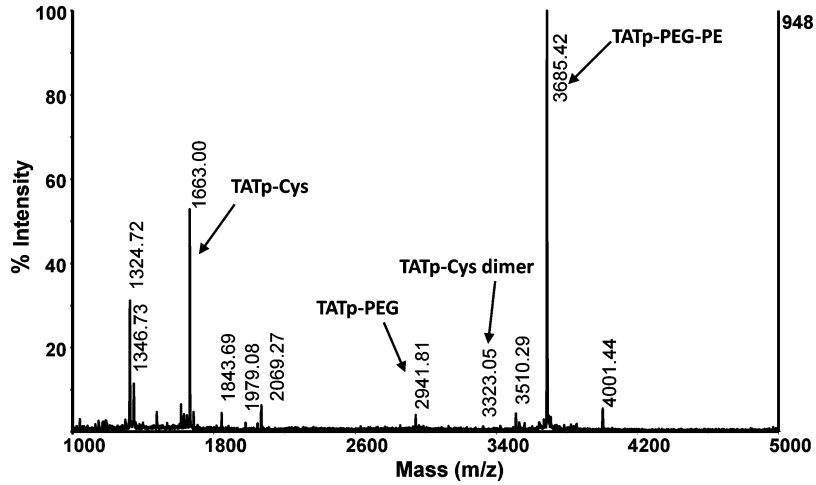

Figure 1. MS spectra of the purified TATp-PEG_{1000}-PE conjugate. The main peak $m/z = 3685.42$ was identified as the conjugate (theoretical $[M+H]^+ = 3685.21$).The intensities of MS peaks do not represent a quantitative ratio. The relative concentration of TATp-Cys did not exceed 7% as determined by HPLC analysis.

TATp-PEG_{1000}-PE (TATp-conjugate) was synthesized in-house (see below). 9-Fluorenylmethyl chloroformate (FMOC-Cl) was purchased from Fluka (Switzerland). Trypsin from porcine pancreas (type IX-S, 13 000−20 000 units/mg), and lyophilized human plasma reconstituted by adding the specified volume of deionized water were purchased from Sigma (St. Louis, MO). All other chemicals and solvents were of analytical grade.

Synthesis of TATp-PEG_{1000}-PE (TATp-Conjugate). TATp-PEG_{1000}-PE conjugate was synthesized as described previously in ref 34 with some modifications. Briefly, an approximately 1.5-fold molar excess of NHS-PEG_{1000}-maleimide was reacted with DOPE-NH_2 by stirring for 4 h in chloroform under argon at room temperature with a 3-fold molar excess of triethylamine. A 2-fold molar excess of TATp-Cys was then added, and the reaction was continued with stirring under argon for an additional 12 h. The excess of TATp-Cys was separated from the product by gel filtration chromatography. The solvent was evaporated, and the product was freeze−dried overnight. The dried product was dissolved in 0.5 mL of water and loaded onto a Sephadex G25 column (length, 10−15 cm; diameter, 0.5−1 cm). The product was eluted with water. Fractions of 0.5−1 mL were collected and monitored by TLC using silica plates and a mobile phase of chloroform/methanol (80:20% v/v). TATp-PEG-PE was visualized by iodine, phosphomolybdic acid, and Dragendorff spray reagents.

The resulting product was freeze−dried, dissolved in chloroform, and stored at −80 °C. The final purified product was identified by MALDI-TOF MS (Figure 1), and its purity as determined by HPLC was above 90%.

Preparation of TATp-Micelles. PEG-PE micelles containing 2.5 mol % of TATp-PEG-PE (TATp-Mic) were prepared as follows: 0.5 mL of PEG_{5000}-PE (10 mg/mL in chloroform) was mixed with 40 μL of TATp-PEG_{1000}-PE (2 mg/mL in chloroform); a PEG-PE film was formed on the bottom of the glass test tube by evaporating the solvent with nitrogen and lyophilization overnight. The film was hydrated in 0.5 mL of PBS, pH 7.4, and vortexed for 2−3 min to yield a clear micelle solution.

A solution of TATp-PEG_{1000}-PE was prepared by a similar procedure, by taking an appropriate volume of the pure TATp-conjugate solution in chloroform (2 mg/mL), evaporating the solvent, and hydrating the residue in PBS, pH 7.4. The hydration required occasional heating to 37 °C and vortexing. Solutions with a conjugate concentration of 0.1 or 1.0 mg/mL were prepared.

Table 1. Summary of the Main Fragments Resulting from Free TATp (0.1 mg/mL) Incubated in Human Plasma at 37 °C, as Identified by MALDI-TOF MS Analysis

incubation time (min)	residual intact TATp YGRKKRRQRRR	main fragments
10	25%	GRKKRRQ**RRR**
		GRKKRRQ**RR**
		GRKKRRQ**R**
		YGRKKRRQ**R**
30	12%	GRKKRRQ**RRR**
		GRKKRRQ**RR**
		GRKKRRQ**R**
		YGRKKRRQ**RR**
		YGRKKRRQ**R**

TATp Proteolysis in Human Plasma. Plasma samples (100 μL) were spiked with 10 μL of TATp (1 mg/mL, in deionized water) and incubated at 37 °C. To follow the kinetics of TATp proteolysis, the incubation was terminated at specified time points by adding 100 μL of acetone with 2% (v/v) of formic acid. The precipitated proteins were separated by centrifugation (10 000 rpm/10 min); the clear supernatant was lyophilized, dissolved in 100 μL of 0.1% formic acid, and filtered through Amicon centrifugal filters (5 kDa MWCO). The resulting filtrate was transferred for MS analysis. The initial concentration of the intact TATp (at time = 0) was determined by adding 10 μL of the same stock (1 mg/mL) of TATp to plasma in which the proteolytic activity was totally inhibited by phenylmethylsulfonyl fluoride (PMSF).

Trypsinolysis of TATp, TATp-PE-PE, and TATp-Mic. Five microliters of trypsin (0.002 mg/mL, 1.5−1.8 total units) was added to a sample of 100 μL of TATp, TATp-PEG-PE, or TATp-Mic in PBS, pH 7.4, and incubated at 37 °C. The concentration of the different forms of TATp was adjusted to be equivalent to 0.05 mg/mL of TATp (3×10^{-5} M), while the final trypsin concentration was 1×10^{-4}mg/mL (5×10^{-9} M). At prescheduled time intervals, 10 μL aliquots were withdrawn from the sample and immediately used for FMOC-Cl derivatization (see below). It was confirmed that trypsin was completely deactivated by the derivatization conditions, (raising the pH to 10 and 1:1 dilution with FMOC-Cl in acetonitrile). The proteolysis kinetics were determined with HPLC analysis by following the increase in the concentration of the main digest product, the RR fragment.

MS Analysis. The samples resulting from the HPLC or plasma filtrates were spiked with human Glu-fibrinopeptide B to serve as an internal standard for the normalization of signal

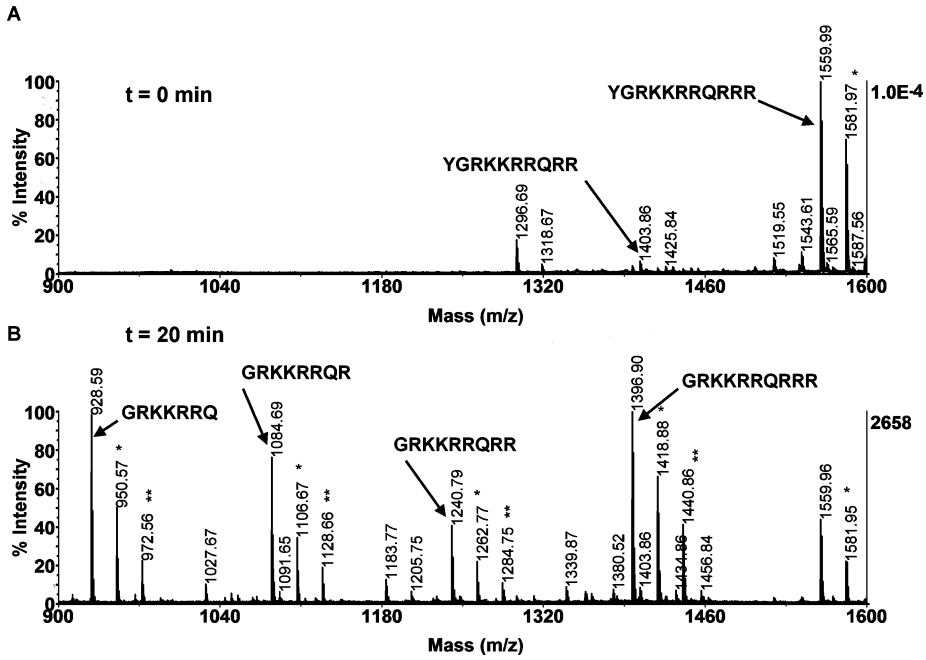

Figure 2. MS spectra of TATp fragments resulting from the incubation of TATp in human plasma at 37 °C. Symbols: * $[M + Na]^+$ and ** $[M + 2Na - H]^+$. (A) $t = 0$ min (determined by spiking TATp into plasma, in which the proteolytic activity was completely inhibited). (B) $t = 20$ min (small peptide fragments were not identified, as they could not be distinguished from the background plasma peptides).

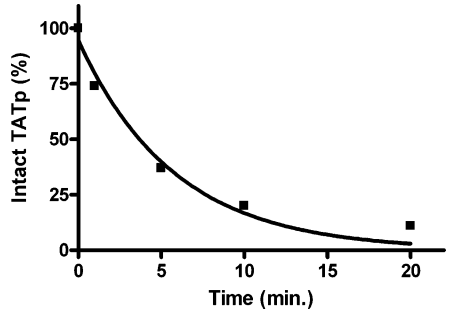

Figure 3. The kinetic of TATp proteolysis in human plasma, described by pseudo-first-order kinetics; $y = 94.84e^{-0.173t}$ ($y = \%$ of residual intact TATp); $R^2 = 0.975$.

intensities. Samples were analyzed by MALDI-TOF-MS in a positive reflectron mode with an AB 4700 instrument (Applied Biosystems, Framingham, MA) using 7 mg/mL α-cyano-4-hydroxycinnamic acid or 2,5-dihydroxybenzoic acid in 50% acetonitrile with 0.1% trifluoroacetic acid in water as a matrix solution. The intensity of TATp signal was expressed as a ratio of TATp peak height over the peak height of the spiked standard. For the identification of the chromatographic peaks by MALDI-TOF-MS analysis, the appropriate fractions were collected, lyophilized, and redissolved in 10 μL of 0.1% formic acid.

TATp Derivatization with FMOC-Cl. Samples of TATp, TATp-PEG-PE, TATp-Mic (10 μL), or their trypsin digests in PBS, pH 7.4, were added to a microcentrifuge tube (0.6 mL) containing 2.5 μL of borate buffer (0.4 M, pH 10) followed by addition of 12.5 μL of FMOC-Cl (0.02−0.4 mg/mL) in acetonitrile, then vortexed and incubated for 10 min at room temperature to complete the derivatization. The FMOC-Cl concentration was adjusted in proportion to that of TATp to reach a molar ratio of 1.2–5. Higher excess of FMOC-Cl should be avoided, as highly derivatized TATp tends to aggregate. The 0.4 mg/mL solution of FMOC-Cl was used with trypsin digest samples. Following the fluorescent labeling, the TATp samples were analyzed by HPLC.

HPLC Analysis. The HPLC analysis was performed on a Hitachi Elite Lachrom system (Tokyo, Japan) composed of the

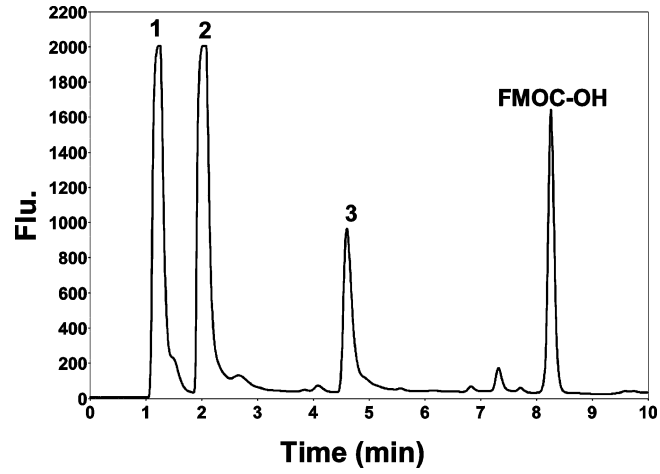

Figure 4. HPLC chromatogram of TATp following FMOC-Cl derivatization. The three separate peaks represent a different extent of derivatization as identified by MALDI-TOF MS (see Figure 5).

following units: a quaternary pump, model L-2130; an automatic sample injector model L-2200; a fluorescence detector, model L-2485, and a Teledyne ISCO fraction collector, Foxy Jr (Lincoln, NE). *EZChrom Elite* (Agilent, Pleasanton, CA) data software was used for the system operation and data processing. The chromatographic separation was performed on a reverse-phase column (Symmetry C18 5 μm, 4.6 × 150 mm, Waters, Milford, MA) using a binary gradient elution. Mobile phase A consisted of 0.1% formic acid in acetonitrile, and B consisted of 0.1% formic acid in deionized water. A constant flow rate of 1 mL/min was used to increase phase A from 30% to 90% within 10 min; this composition (90% A) was held for 5 min and then changed back to the initial composition (30% A). A wait for an additional 5 min was allowed for the column to equilibrate to the initial eluent composition. The FMOC-Cl derivatized samples were diluted 20- to 100-fold with deionized water, and 10 μL volumes were injected for analysis. The

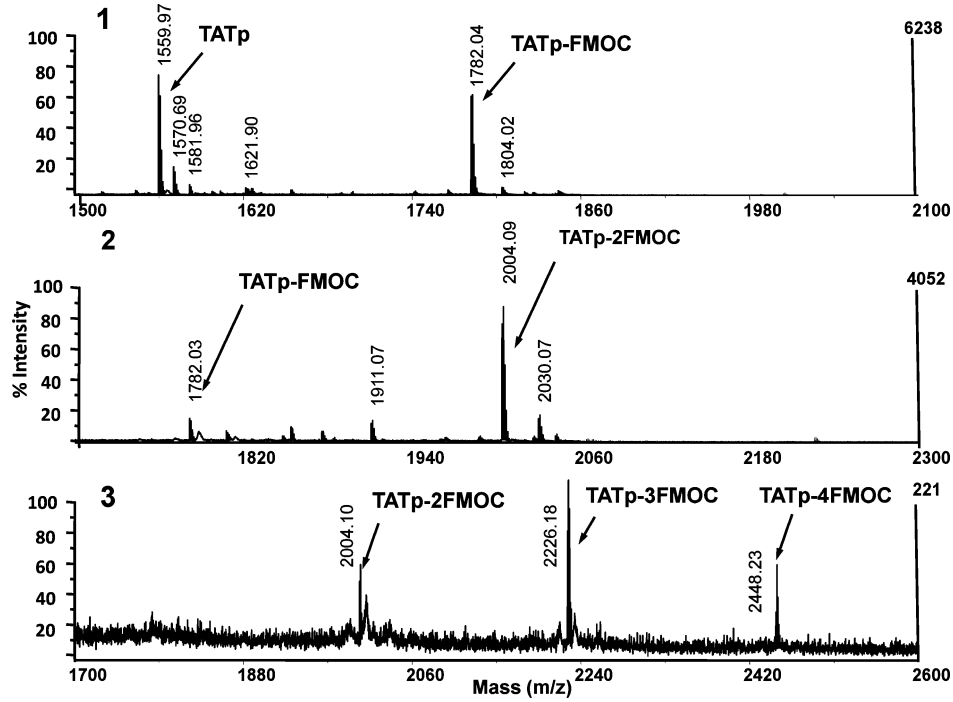

Figure 5. MS identification of the relevant peaks 1−3 (see Figure 4) resulting from FMOC derivatization of TATp. 1, TATp-FMOC and nonderivatized TATp; 2, TATp-2FMOC and traces of TATp-FMOC; 3, TATp-3FMOC and traces of TATp-2FMOC and TATp-4FMOC.

precolumn labeled analytes were detected by the fluorescence detector (ex 263 nm, em 314 nm).

RESULTS

TATp Proteolysis in Human Plasma. The kinetics of TATp proteolysis in human plasma were studied by MALDI-TOF-MS analysis. The main fragments resulting from TATp cleavage were identified as depicted in Figure 2 and summarized in Table 1. The same main fragments were found after 10 and 30 min of plasma incubation, but there was a pronounced change in their relative intensities. The ratio between the most intense fragment resulting from the N-terminal cleavage (GRKKRRQR-RR) and the fragment resulting from C-terminal cleavage (YGRKKRRQRR) increased by 3-fold after 30 min. There was also an increase in the intensity of the smaller fractions with incubation time.

The kinetics of TATp proteolysis were determined by MS analysis by following the decrease in the concentration of the intact TATp as a function of time. As found in other works on peptide proteolysis (*33*), the resulting kinetics (Figure 3) followed a pseudo-first-order rate, described by the following equation: $y = b \cdot e^{-kt}$, where y is the normalized concentration (percentage) of the residual intact peptide at time t; b, the initial peptide concentration; k, the pseudo-first-order rate constant, and t, the incubation time in minutes. The half-life ($t_{1/2}$) calculated from the resulting rate constant equaled 3.5 min. This result points out that the expected lifetime of nonprotected TATp *in vivo* should be on the scale of few minutes.

HPLC Method for TATp Analysis. The analytical method based on HPLC we have developed, with the use of precolumn FMOC derivatization (*35*), RP-chromatography, and fluorescence detection, proved to be a fast and highly sensitive analytical tool to study the proteolytic digestion of TATp.

TATp contains four functional groups which can readily react with FMOC-Cl, three primary amino groups—one at the N-terminal and two at the R-chains of lysine—and the phenol group on tyrosine. As a result, several derivatization products are expected. We found such products separated by HPLC into three peaks (Figure 4) and identified by MS as containing one, two, three, and four FMOC labels per TATp molecule (Figure 5). The FMOC labeling extent could be controlled by adjusting the quantity of the FMOC-Cl used for the derivatization. High molar excesses of FMOC-Cl should be avoided since the highly derivatized peptide tends to aggregate.

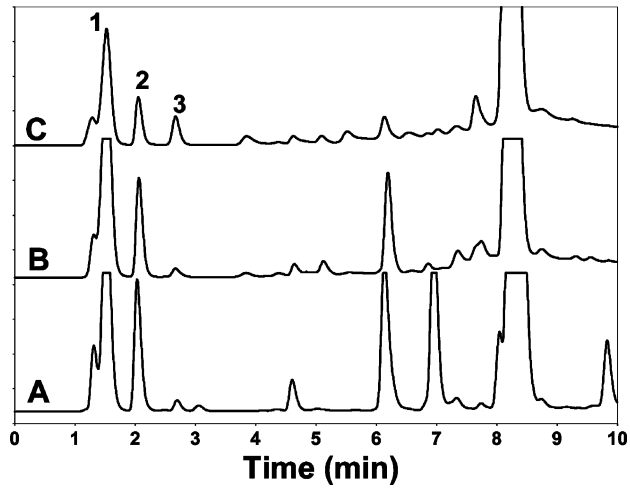

Figure 6. HPLC chromatograms of TATp fragments resulting from the trypsinolysis (1.5 trypsin unit/mL) for 20 min in PBS, pH 7.4, at 37 °C. For the proteolysis of TATp-Mic, 100-fold higher concentration of trypsin was used. Fractions of peaks 1, 2, and 3 were collected and identified by MS. The chromatograms represent free TATp (A), TATp-conjugate (B), TATp-Mic (C).

We found the main derivatization product to be TATp-FMOC, when a molar ratio (FMOC/TATp) of 1.2 was used, and TATp-3FMOC, when a molar ratio of 4.8 was used.

TATp Trypsinolysis in PBS, pH 7.4. For the *in vitro* studies of the proteolysis kinetics of TATp, TATp-conjugate, and TATp-Mic, a solution of trypsin (1×10^{-4} mg/mL, 1.5−1.8 units/mL) in PBS, pH 7.4, was used. This trypsin concentration allowed for TATp proteolysis kinetics similar to those found in human plasma. By using the HPLC analysis to follow the proteolysis of TATp, the same main peptide fragments, peaks

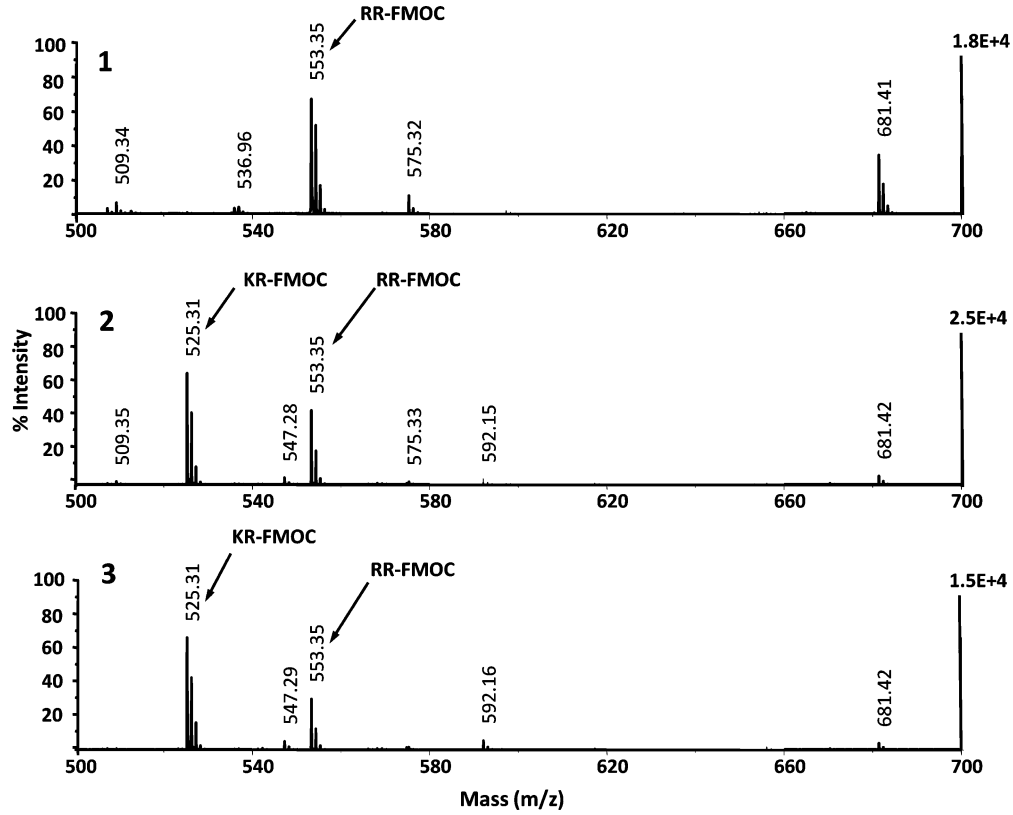

Figure 7. MS identification of the three main fractions (1−3) resulting from TATp proteolysis: (1) RR-FMOC, (2) KR-FMOC, (3) KR-FMOC. The two separate chromatographic peaks of KR-FMOC might result from the two different positions of FMOC labeling: N-terminal or ε-amino group of lysine.

1, 2, and 3 (Figure 6) were detected for the three (A,B,C) different forms of TATp used in this study. The fractions were identified by MS (Figure 7), fraction 1 as RR, and fractions 2 and 3 as KR with individual chromatographic peaks for KR resulting from different positions of FMOC labeling (at N-terminus or ε-amino groups). The RR dimer was the predominant initial proteolysis fragment, which is believed to result from the endocleavage at the carboxyl terminus (YGRKKRRQR↓RR). This finding is in agreement with the cleavage of TATp by furin (*28*).

We found that the chromatographic peak of the RR fragment was the most suitable for the proteolysis kinetics studies since it was the most intense initial fragment and thus easy to detect and analyze quantitatively.

The proteolysis kinetics of TATp were studied either by following the decrease in intact TATp as a function of the incubation time or by following the increase in the main digest fragment (RR). Similar kinetic rates were obtained with both methods (Figure 8). We preferred, however, the method based on the RR fragment, since the same peptide fragment (RR) was found to be the main proteolysis product for all three forms of TATp used in this study. This enabled us to use precisely the same HPLC method for the proteolysis kinetics determination of all the different forms of TATp.

The proteolysis kinetics as determined for the different forms of TATp (Figure 9) fit pseudo-first-order kinetics (R^2 = 0.94−0.98) well, although with quite different proteolysis rates as expressed by the half-lives of TATp: 3.5, 10, and 430 min for TATp, TATp-conjugate, and TATp-Mic, respectively.

DISCUSSION

The studies of the proteolysis of TATp represented in the present work are based on highly precise analytical tools: MALDI-TOF-MS and HPLC. We believe it was important to develop an HPLC method for this study in addition to the MS since most laboratories do not have free access to costly MS instruments. The HPLC analysis developed in this work proved to be a straightforward, highly sensitive, and accurate analytical tool to study the proteolysis kinetics of TATp and TATp conjugates incorporated into PEGylated micelles.

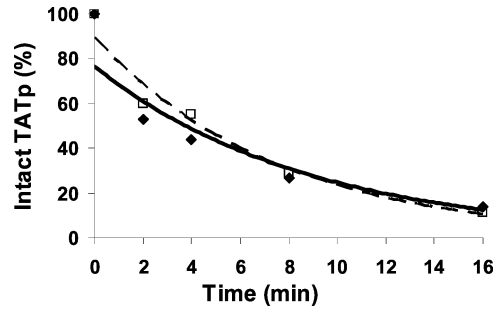

Figure 8. The kinetics of TATp proteolysis by trypsin (1.5 units/mL) in PBS, pH 7.4, at 37 °C. The kinetics was followed by the HPLC based on two different monitoring methods: 1. (—) By determining the decrease in the concentration of the intact TATp. 2. (---) By determining the increase of the RR-fragment normalized to % of the residual intact TATp using the following equation: % Intact TATp = $[A_\infty - A_t/A_\infty] \times 100$; A_∞ = RR concentration at the end of proteolysis; At = RR concentration at time t. The kinetics as determined by both methods fit first-order kinetics (as specified in Figure 2) resulting in a similar half-life ($t_{1/2}$ = ca. 3.5 min).

These kinetics results point out that the expected lifetime *in vivo* of the nonprotected TATp should be on the scale of a few minutes, while highly protected TATp in TATp-Mic can be expected to have a lifetime of several hours. The pronounced differences in the stability against proteolysis among TATp, TATp-conjugate, and TATp-Mic are quite understandable when their structural differences in aqueous medium are taken into

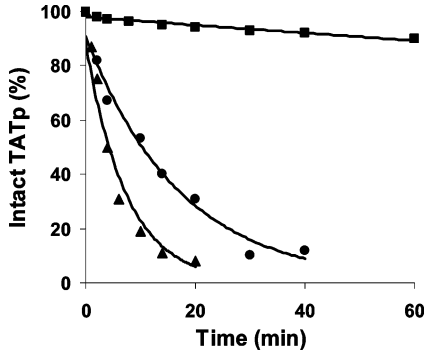

Figure 9. Proteolysis kinetics of different forms of TATp by trypsin (1.5 units/mL) in PBS, pH 7.4, 37 °C, following the RR fragment (as specified in Figure 8). TATp (▲), TATp-conjugate (•), TATp-Mic (■).

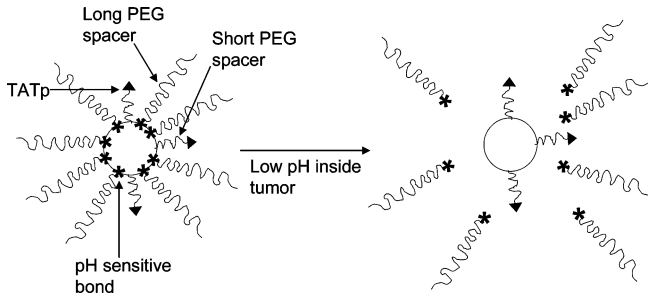

Figure 10. The principal scheme for the action of stimuli-sensitive nanocarriers. The surface of the nanocarrier is modified with TATp (or other CPP) via a relatively short PEG spacer. The TATp is shielded with longer PEG chains, which are attached to the nanocarrier surface via pH-sensitive bonds. The whole system is stable in the blood with TATp moieties protected against proteolytic degradation, and the carrier accumulates in the tumor via the EPR effect. Inside the tumor, protective PEG chains are detached from the surface by rapid hydrolysis of pH-sensitive bonds at the lower intratumoral pH; intact TATp becomes exposed and allows TATp-mediated intracellular delivery.

account. Free TATp can be attacked easily by trypsin and degraded rapidly. The TATp-PEG-PE conjugate, a clearly amphiphilic molecule, can exist in solution as an individual molecule or can form micelles similar to PEG-PE (we did not study the detailed properties of these micelles), but both in free form and in such micelles, the TATp moiety is exposed to the water phase and can still be attacked by trypsin. To some extent, certain steric hindrances for such attacks are created by the presence of PEG or by the micelle surface and will slow down the degradation rate (half-life increased from 3 min for free TATp to 10 min for the TATp-conjugate). By contrast, in TATp-Mic, where the TATp-PEG_{1000}-PE conjugate is located between PEG_{5000}-PE chains, the extended PEG_{5000} chains sterically protect the TATp moiety hidden inside the hydrophilic corona of the mixed micelle from the enzymatic attack and result in a greatly increased lifetime of TATp in TATp-Mic.

These attempts being made to construct "smart" drug delivery systems involve a TATp function hidden under a PEG-based shield, which could be removed, exposing their cell-penetrating function only when the system was in the vicinity of target cells (*22, 34, 36*) as depicted in Figure 10. The findings presented clearly show that the hidden TATp function can be well preserved within such "smart" structures for the time required for drug delivery into a target.

CONCLUSIONS

The HPLC analysis based on the FMOC-Cl fluorescent labeling developed in this work is a straightforward, accurate analytical tool for studying the proteolysis kinetics of TATp and TATp conjugates incorporated into PEGylated micelles.

The proteolytic cleavage of free TATp in human plasma or in trypsin-containing medium is relatively fast, with a half-life of approximately 3.5 min. TATp modification with PEG-PE moieties stabilizes TATp only slightly against proteolytic degradation ($t_{1/2}$ = 10 min). High stability of TATp against proteolysis ($t_{1/2}$ > 400 min) can be achieved by incorporating TATp as TATp-PEG-PE conjugates into polymeric micelles formed by PEG-PE if the size of a PEG block is bigger than the PEG fragment in TATp-PEG-PE. Protection of TATp against proteolysis is of great importance for its potential use as a cell-penetrating moiety in multifunctional smart drug delivery systems.

ACKNOWLEDGMENT

This study was supported by the NIH grants RO1 CA121838 and RO1 CA128486 to VPT. W.C. Hartner is gratefully acknowledged for his help during this manuscript preparation.

LITERATURE CITED

(1) Frankel, A. D., and Pabo, C. O. (1988) Cellular uptake of the tat protein from human immunodeficiency virus. *Cell 55*, 1189–1193.

(2) Fawell, S., Seery, J., Daikh, Y., Moore, C., Chen, L. L., Pepinsky, B., and Barsoum, J. (1994) Tat-mediated delivery of heterologous proteins into cells. *Proc. Natl. Acad. Sci. U.S.A. 91*, 664–668.

(3) Schwarze, S. R., Ho, A., Vocero-Akbani, A., and Dowdy, S. F. (1999) In vivo protein transduction: delivery of a biologically active protein into the mouse. *Science 285*, 1569–1572.

(4) Ryser, H. J., and Hancock, R. (1965) Histones and basic polyamino acids stimulate the uptake of albumin by tumor cells in culture. *Science 150*, 501–503.

(5) Goun, E. A., Pillow, T. H., Jones, L. R., Rothbard, J. B., and Wender, P. A. (2006) Molecular transporters: synthesis of oligoguanidinium transporters and their application to drug delivery and real-time imaging. *ChemBioChem 7*, 1497–1515.

(6) Chauhan, A., Tikoo, A., Kapur, A. K., and Singh, M. (2007) The taming of the cell penetrating domain of the HIV Tat: myths and realities. *J. Controlled Release 117*, 148–162.

(7) Fischer, R., Kohler, K., Fotin-Mleczek, M., and Brock, R. (2004) A stepwise dissection of the intracellular fate of cationic cell-penetrating peptides. *J. Biol. Chem. 279*, 12625–12635.

(8) Dathe, M., Schumann, M., Wieprecht, T., Winkler, A., Beyermann, M., Krause, E., Matsuzaki, K., Murase, O., and Bienert, M. (1996) Peptide helicity and membrane surface charge modulate the balance of electrostatic and hydrophobic interactions with lipid bilayers and biological membranes. *Biochemistry 35*, 12612–12622.

(9) Ryser, H. J. (1968) Uptake of protein by mammalian cells: an underdeveloped area. The penetration of foreign proteins into mammalian cells can be measured and their functions explored. *Science 159*, 390–396.

(10) Fuchs, S. M., and Raines, R. T. (2004) Pathway for polyarginine entry into mammalian cells. *Biochemistry 43*, 2438–2444.

(11) Ignatovich, I. A., Dizhe, E. B., Pavlotskaya, A. V., Akifiev, B. N., Burov, S. V., Orlov, S. V., and Perevozchikov, A. P. (2003) Complexes of plasmid DNA with basic domain 47−57 of the HIV-1 Tat protein are transferred to mammalian cells by endocytosis-mediated pathways. *J. Biol. Chem. 278*, 42625–42636.

(12) Rothbard, J. B., Jessop, T. C., Lewis, R. S., Murray, B. A., and Wender, P. A. (2004) Role of membrane potential and hydrogen bonding in the mechanism of translocation of guanidinium-rich peptides into cells. *J. Am. Chem. Soc. 126*, 9506–9507.

(13) Wadia, J. S., Stan, R. V., and Dowdy, S. F. (2004) Transducible TAT-HA fusogenic peptide enhances escape of TAT-fusion proteins after lipid raft macropinocytosis. *Nat. Med. 10*, 310–315.
(14) Silhol, M., Tyagi, M., Giacca, M., Lebleu, B., and Vives, E. (2002) Different mechanisms for cellular internalization of the HIV-1 Tat-derived cell penetrating peptide and recombinant proteins fused to Tat. *Eur. J. Biochem. 269*, 494–501.
(15) Stein, S., Weiss, A., Adermann, K., Lazarovici, P., Hochman, J., and Wellhoner, H. (1999) A disulfide conjugate between anti-tetanus antibodies and HIV (37−72)Tat neutralizes tetanus toxin inside chromaffin cells. *FEBS Lett. 458*, 383–386.
(16) De Coupade, C., Fittipaldi, A., Chagnas, V., Michel, M., Carlier, S., Tasciotti, E., Darmon, A., Ravel, D., Kearsey, J., Giacca, M., and Cailler, F. (2005) Novel human-derived cell-penetrating peptides for specific subcellular delivery of therapeutic biomolecules. *Biochem. J. 390*, 407–418.
(17) Lee, H. J., and Pardridge, W. M. (2001) Pharmacokinetics and delivery of tat and tat-protein conjugates to tissues in vivo. *Bioconjugate Chem. 12*, 995–999.
(18) Torchilin, V. P., Levchenko, T. S., Rammohan, R., Volodina, N., Papahadjopoulos-Sternberg, B., and D'Souza, G. G. (2003) Cell transfection in vitro and in vivo with nontoxic TAT peptide-liposome-DNA complexes. *Proc. Natl. Acad. Sci. U.S.A. 100*, 1972–1977.
(19) Ziegler, A., and Seelig, J. (2007) High affinity of the cell-penetrating peptide HIV-1 Tat-PTD for DNA. *Biochemistry 46*, 8138–8145.
(20) Torchilin, V. P., Rammohan, R., Weissig, V., and Levchenko, T. S. (2001) TAT peptide on the surface of liposomes affords their efficient intracellular delivery even at low temperature and in the presence of metabolic inhibitors. *Proc. Natl. Acad. Sci. U.S.A. 98*, 8786–8791.
(21) Gupta, B., Levchenko, T. S., and Torchilin, V. P. (2007) TAT peptide-modified liposomes provide enhanced gene delivery to intracranial human brain tumor xenografts in nude mice. *Oncol. Res. 16*, 351–359.
(22) Kale, A. A., and Torchilin, V. P. (2007) "Smart" drug carriers: PEGylated TATp-modified pH-sensitive liposomes. *J. Liposome Res. 17*, 197–203.
(23) Koch, A. M., Reynolds, F., Kircher, M. F., Merkle, H. P., Weissleder, R., and Josephson, L. (2003) Uptake and metabolism of a dual fluorochrome Tat-nanoparticle in HeLa cells. *Bioconjugate Chem. 14*, 1115–1121.
(24) Ruan, G., Agrawal, A., Marcus, A. I., and Nie, S. (2007) Imaging and tracking of tat peptide-conjugated quantum dots in living cells: new insights into nanoparticle uptake, intracellular transport, and vesicle shedding. *J. Am. Chem. Soc. 129*, 14759–14766.
(25) Endres, P. J., Macrenaris, K. W., Vogt, S., Allen, M. J., and Meade, T. J. (2006) Quantitative imaging of cell-permeable magnetic resonance contrast agents using x-ray fluorescence. *Mol. Imaging 5*, 485–497.
(26) Vives, E., Brodin, P., and Lebleu, B. (1997) A truncated HIV-1 Tat protein basic domain rapidly translocates through the plasma membrane and accumulates in the cell nucleus. *J. Biol. Chem. 272*, 16010–16017.
(27) Siomi, H., Shida, H., Maki, M., and Hatanaka, M. (1990) Effects of a highly basic region of human immunodeficiency virus Tat protein on nucleolar localization. *J. Virol. 64*, 1803–1807.
(28) Tikhonov, I., Ruckwardt, T. J., Berg, S., Hatfield, G. S., and David Pauza, C. (2004) Furin cleavage of the HIV-1 Tat protein. *FEBS Lett. 565*, 89–92.
(29) Trehin, R., Nielsen, H. M., Jahnke, H. G., Krauss, U., Beck-Sickinger, A. G., and Merkle, H. P. (2004) Metabolic cleavage of cell-penetrating peptides in contact with epithelial models: human calcitonin (hCT)-derived peptides, Tat(47−57) and penetratin(43−58). *Biochem. J. 382*, 945–956.
(30) Elmquist, A., and Langel, U. (2003) In vitro uptake and stability study of pVEC and its all-D analog. *Biol. Chem. 384*, 387–393.
(31) Schorderet, D. F., Manzi, V., Canola, K., Bonny, C., Arsenijevic, Y., Munier, F. L., and Maurer, F. (2005) D-TAT transporter as an ocular peptide delivery system. *Clin. Experiment. Ophthalmol. 33*, 628–635.
(32) Achilefu, S., Srinivasan, A., Schmidt, M. A., Jimenez, H. N., Bugaj, J. E., and Erion, J. L. (2003) Novel bioactive and stable neurotensin peptide analogues capable of delivering radiopharmaceuticals and molecular beacons to tumors. *J. Med. Chem. 46*, 3403–3411.
(33) Meng, H., and Kumar, K. (2007) Antimicrobial activity and protease stability of peptides containing fluorinated amino acids. *J. Am. Chem. Soc. 129*, 15615–15622.
(34) Kale, A. A., and Torchilin, V. P. (2007) Enhanced transfection of tumor cells in vivo using "Smart" pH-sensitive TAT-modified pegylated liposomes. *J. Drug Targeting 15*, 538–545.
(35) Lewis, J. R., Morley, J. S., and Venn, R. F. (1993) Analysis of human beta-endorphin 28−31 (melanotropin potentiating factor) and analogues by high-performance liquid chromatography of their 9-fluorenylmethoxycarbonyl derivatives. *J. Chromatogr. 615*, 37–45.
(36) Sawant, R. M., Hurley, J. P., Salmaso, S., Kale, A., Tolcheva, E., Levchenko, T. S., and Torchilin, V. P. (2006) "SMART" drug delivery systems: double-targeted pH-responsive pharmaceutical nanocarriers. *Bioconjugate Chem. 17*, 943–949.

BC900081E